

Expanding the Toolbox of Upconversion Nanoparticles for In Vivo Optogenetics and Neuromodulation

Angelo Homyoun All,* Xiao Zeng, Daniel Boon Loong Teh, Zhigao Yi, Ankshita Prasad, Toru Ishizuka, Nitish Thakor, Yawo Hiromu, and Xiaogang Liu*

Optogenetics is an optical technique that exploits visible light for selective neuromodulation with spatio-temporal precision. Despite enormous effort, the effective stimulation of targeted neurons, which are located in deeper structures of the nervous system, by visible light, remains a technical challenge. Compared to visible light, near-infrared illumination offers a higher depth of tissue penetration owing to a lower degree of light attenuation. Herein, an overview of advances in developing new modalities for neural circuitry modulation utilizing upconversion-nanoparticle-mediated optogenetics is presented. These developments have led to minimally invasive optical stimulation and inhibition of neurons with substantially improved selectivity, sensitivity, and spatial resolution. The focus is to provide a comprehensive review of the mechanistic basis for evaluating upconversion parameters, which will be useful in designing, executing, and reporting optogenetic experiments.

1. Introduction

Optogenetics, a technique that uses light as a modality of biological control to manipulate neuronal function, has revolutionized our ability to influence individual neurons and decode neural circuit mechanisms in the nervous system.^[1] This well-controlled active intervention is made possible by transfecting targeted neuromodulatory pathways through genetically encoded light-sensitive opsin proteins. In 2005, Boyden et al. reported the successful *in vitro* transfection and expression of functional channelrhodopsins (ChR) in mammalian neurons with lentiviral gene delivery.^[2] Pulsed-light flashes triggers an inward cation flow and neuron firing patterns whose frequencies matched that of the external stimulus (25 Hz). The fast on–off kinetics and high temporal precision

enable the spontaneous control of synaptic events. This is reproducible at the level of a single neuron. By comparison, pharmacological interventions often show major limitations, including delay responses to the transient level of activity in neurons, as well as relatively defocused electrical stimulations, which render them not preferred modulation methods for targeting single neurons and neuronal circuits.

In practice, visible light in the range of 430–630 nm is typically used to regulate the activities of opsins, which are light-gated ion channels and light-driven ion pumps expressed on the cellular membrane (**Scheme 1**).^[3] The resulting movement of different positively and negatively charged ions through the membrane protein opsins will either depolarize or hyperpolarize the genetically transfected neurons, which will result in stimulation or inhibition of neuronal function, respectively. Optogenetics enables almost instantaneous response of opsins to visible light along with the benefits of pinpoint optical targeting and high spatiotemporal resolution. This highly rapid and selective neuromodulation by visible light is not possible by any other modalities, such as electrical or magnetic stimulation. In addition, optogenetics provide a powerful platform to investigate the cell-type specificity, the relationship among neuronal activities, and behavior correlation.

In performing optogenetic neuromodulation to study *in vivo* behavior in rodents, absorption and scattering of visible light by neuronal tissues are two major limiting factors.^[4] Obviously, light scattering poses a significant constraint on delivering

Prof. A. H. All, Prof. N. Thakor
Department of Biomedical Engineering & Department of Neurology
Johns Hopkins School of Medicine
Baltimore, MD 21205, USA
E-mail: hmn@jhu.edu

Dr. X. Zeng, Z. Yi, Prof. X. Liu
Department of Chemistry
National University of Singapore
Singapore 117543, Singapore
E-mail: chmlx@nus.edu.sg

Dr. D. B. L. Teh, Prof. N. Thakor
Department of Medicine & Singapore Institute for Neurotechnology (SINAPSE)
National University of Singapore
Singapore 117456, Singapore

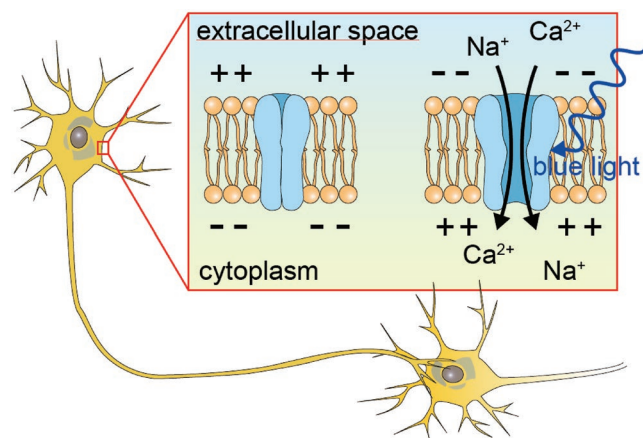
Dr. A. Prasad, Prof. N. Thakor
Department of Biomedical Engineering
National University of Singapore
Singapore 117583, Singapore

Prof. T. Ishizuka, Prof. Y. Hiromu
Department of Integrative Life Sciences
Tohoku University Graduate School of Life Sciences
Sendai 980-8577, Japan

Prof. X. Liu
Center for Functional Materials
National University of Singapore Suzhou Research Institute
Suzhou, Jiangsu 215123, China

 The ORCID identification number(s) for the author(s) of this article can be found under <https://doi.org/10.1002/adma.201803474>.

DOI: 10.1002/adma.201803474



Scheme 1. Illustration showing how opsins (ChR2 in this case) respond to light stimulation. In the absence of light, the channel in ChR2 remains closed, prohibiting cations from entering the cytoplasm. The neuron maintains a negative resting potential and remains inactivated. In contrast, in response to blue-light illumination, ChR2 opens its channel and allows an inward cation flux. The current generated by the cation flux depolarizes the membrane of the neuron. Once the membrane potential is raised from ≈ -70 to -50 mV, the neuron fires an action potential that propagates to adjacent neurons.

visible light into the deeper structures of the nervous system. One solution is to implant an optical fiber that is tethered to a remote laser in the brain for the efficient delivery of light to multiple targets inside the brain.^[5] However, the implanted fiber often creates a tangible debilitating force that may cause significant brain injury and impede the animal's free movement. In addition, the movement of the animal may lead to fiber displacement and cause further damage to brain tissue. Other options involve head-mounted optical systems, but with a very limited depth of light penetration and a considerable constraint over the movement of the animal due to the wiring or a restrictive tether.^[6] Therefore, development of a wireless and noninvasive neuronal optical manipulation system capable of creating a light source deep within the nervous tissue is highly desirable. A fully wireless noninvasive system would enable chronic monitoring of awake animals and will enable long-term longitudinal experimentation.

Conventionally, optogenetics uses visible light in the blue or amber spectral bands. However, visible light does not penetrate deep into biological tissues. By comparison, red and near-infrared (NIR) light beams have lower absorption rate and can travel deeper into neuronal (brain) tissues than blue and green light.^[7] In addition, employing opsins that are responsive to orange or red light in optogenetic studies allows minimally invasive control of animal behaviors by external LED illumination.^[8] However, opsin variants that are highly sensitive to the far-red and NIR light have yet to be effectively engineered. This restriction limits the precise modulation of neurons in the deeper regions of the brain. Nevertheless, recently, red-activatable ChR (ReaChR), which has an optimal excitation between the orange to red light wavelength (590–655 nm), has been developed.^[8] ReaChR has improved the level of membrane trafficking and expression as compared to the previously reported redshifted opsins such as VChR1.^[9]



Angelo All started his higher education in pharmacy school (University of Bologna, Italy), graduated from medical school (University of Verona, Italy), continued his career as an intern surgeon (Policlinic Hospital, Verona, Italy), and obtained an MBA degree in Healthcare Management (Johns Hopkins University).

Currently he is a primary faculty member at the Department of Biomedical Engineering, Division of Neuroscience and Neuroengineering, Johns Hopkins School of Medicine (Baltimore, USA). The focus of his research is nervous system injury, repair and regeneration. His translational research projects involve stem cell replacement therapy, neuro-electrophysiology, plasticity, and optomedicine, which is a novel optogenetics-based approach application of upconversion nanoparticles for neuromodulation as well as rehabilitative treatment post-neuronal injury.



Xiaogang Liu earned his B.E. degree (1996) in chemical engineering from Beijing Technology and Business University, P. R. China. He received his M.S. degree (1999) in chemistry from East Carolina University and completed his Ph.D. (2004) at Northwestern University. After completing his post-doctoral training at MIT, he

joined the faculty of the National University of Singapore in 2006. His research encompasses optical nanomaterials and energy transfer and explores the use of luminescent nanocrystals for photocatalysis, sensing, and biomedical applications.

Interestingly, through intact skin and the skull, the expression of ReaChR in mouse vibrissae motor cortex (vM1) evoked vibrissae movement in response to excitation at 655 nm. The noninvasive control of vibrissae was further demonstrated in the brainstem activation of vibrissa motoneurons by LED excitation through the auditory canal. However, the ReaChR falls short as a slower kinetics for their “channel rate of closing” properties as compared to ChR2.^[10] Moreover, Chrimson, a more far-redshifted ChR, which has been successfully activated upon excitation at 735 nm, shows an optimal absorption wavelength of 660 nm.^[11] However, application of Chrimson is limited by its slow recovery kinetics, which results in inactivation at higher frequencies above 10 Hz. This can be slightly improved with the mutant version known as ChrimsonR,

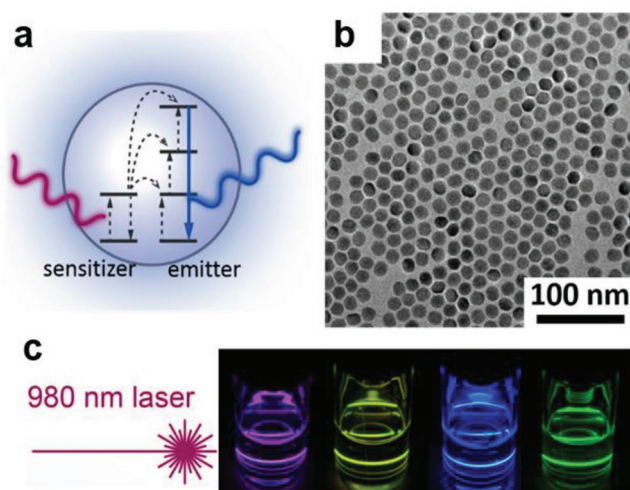


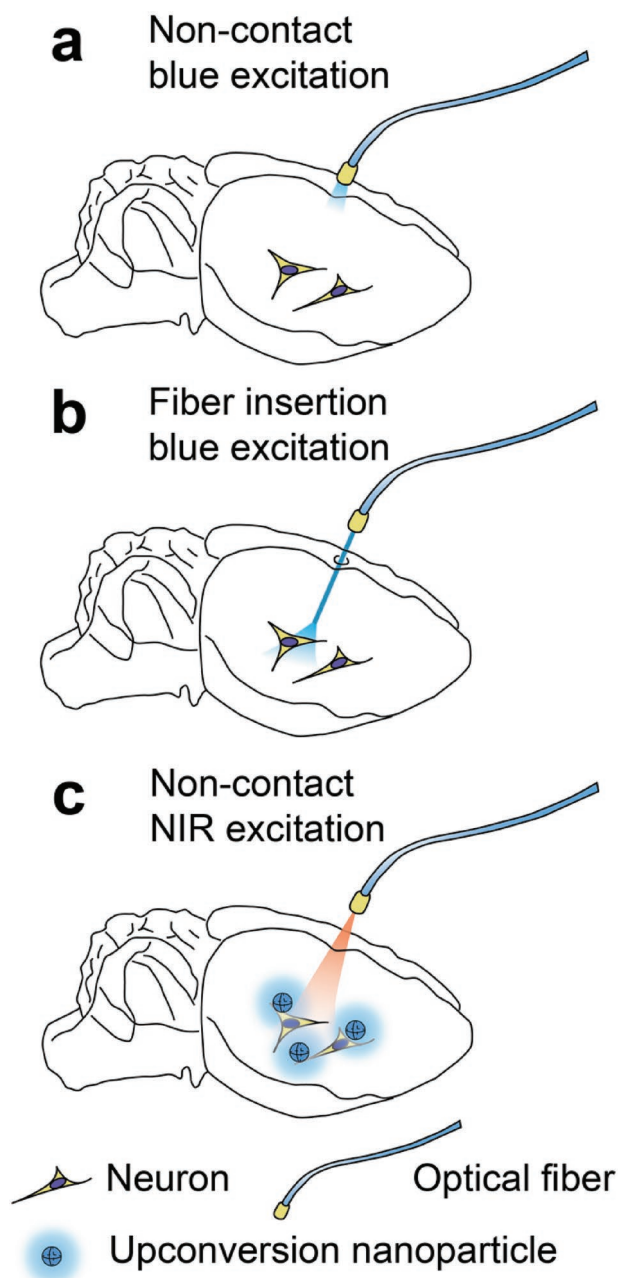
Figure 1. a) Illustration of the energy transfer upconversion mechanism. In an inorganic host matrix, a sensitizer ion absorbs NIR light and sequentially transfers the absorbed energy to a neighboring emitter ion, promoting the emitter to higher-lying energy levels. Subsequent electronic transitions in the emitter ion lead to upconversion emission. b) A representative transmission electron microscopy (TEM) image showing monodispersed UCNPs. c) A photograph showing multicolor upconversion emission under a single 980 nm excitation source.

which enables the stimulation frequency to be expanded larger than 10 Hz.

Although the far-red-activatable opsins allow a better depth of penetration, their absorption usually peaks at $\approx 550\text{--}650\text{ nm}$ and the sensitivity of their absorption is not optimal in the spectral range beyond 700 nm. An alternative method to address the light-delivery challenge in optogenetics is to employ NIR light and subsequently convert it into visible light. In support of this approach, researchers have recently proposed upconversion nanoparticles (UCNPs), a class of nanomaterials that can convert low-energy laser stimulation into high-energy luminescent emissions (Figure 1).^[12] UCNPs function as a mediator to transform highly penetrable NIR light into visible light at a specific wavelength, which is necessary for optogenetic manipulation of neural tissues. This has been considered a powerful tool to advance applications of optogenetics for in vivo models and translational neuroscience research (Scheme 2).^[13]

In theory, implanting UCNPs in close proximity to opsin-expressing neurons would allow NIR illumination to be converted into visible emission efficiently, and would consequently excite ChR light-gated ion channels.^[1,3,5] However, practically, the effective implementation of this design requires careful consideration of many factors including the light-conversion efficiency, the close correlation of visible-light emission wavelength, which needs to exactly match the absorption spectra of ChR, the effect of laser-induced overheating, and the biocompatibility of the nanoparticles.

Our aim here is to review the basic principles and feasibility of NIR-based optogenetics involving UCNPs. We review recent examples of using UCNPs to achieve NIR-light-mediated regulation of neurons and discuss the progress in developing new modalities that facilitate the simultaneous



Scheme 2. Methods of sending light to deep-lying neurons in a mouse brain. a) Noncontact blue excitation through an optical fiber placed slightly above the brain surface. Note that the efficiency of blue-light activation is low due to light scattering. b) Blue excitation through a surgically implanted optical fiber. Although blue light can reach the neurons and evoke action potential firing, this mode of operation may limit the animal's free movement during the experiment and causes tissue damage. c) Noncontact NIR excitation through the use of UCNPs. When placed in the vicinity of the targeted neurons, upconversion materials convert the NIR irradiation into blue light that in turn activates the neurons.

imaging and optical interrogation of different brain regions that are inaccessible to conventional noninvasive techniques. These topics include the fundamental design of experiments and the choice of upconversion nanomaterials, as well as

the detailed results of the visualization and manipulation of neural activity in response to a broad variety of physiological stimuli. Key challenges in controlling cellular function with upconversion-nanoparticle-mediated optogenetics and the likely directions of future research in this emerging field will also be discussed.

2. Overview of Optogenetics

2.1. Optogenetics: A Combination of Gene Targeting and Optics for Cellular Function Modulation

The neural circuitry forms the basis that governs our physiology, including pain sensation, decision making, memory formation, sensory-motor function, and even the levels of glucose in the body. The ability to turn on/off selected groups of neurons with millisecond spatial and temporal precision would allow individual neurons and neural networks to be probed. As such, neuromodulation is critical to understanding the individual neural circuitry functions within the nervous system. In general, optogenetics utilize the exogenous expression of light-sensitive microbial opsins as light-gated ion channels or light-driven ion pumps to alter cellular physiology upon light illumination.^[14] However, in broader terms, the collective regulation of a group of neurons or connected neural networks in the brain structures would be more desirable to reveal the interaction between neural circuitry and animal physiology or behavior.

To fully comprehend the application of optogenetics, one must consider factors involving opsin gene delivery, membrane trafficking and expression, wavelength sensitivity, and light delivery. With proper molecular modification, the opsins can be targeted to the cells of interest.^[15] For applications to neuroscience, transgenic lines of *Cre*-dependent rodents allow opsins to be targeted to specific neural cells.^[16] Alternatively, viral transduction, which requires the localized injection of a viral vector at the region of interest, is another commonly used method for delivering opsin genes into the cells of interest. The specificity of opsin expression in cells can also be achieved by driving the opsin gene with cell-type-specific gene promoters or utilizing unique virus serotype tropism.^[17]

Several unique types of opsins that possess characteristic ionic selectivity, on–off kinetics and wavelength sensitivity have been made available. For instance, Wang et al. demonstrated a shift in spectral sensitivity (a level of membrane expression), desensitization, and turning-off the kinetics when segments of ChR1 and ChR2 were switched to generate different chimeras of ChR.^[18] In contrast to the native ChR, which is a blue-light-gated opsin, VChR1 permits redshifted neural photostimulation but with poor photocurrent output. However, this deficiency can be mitigated by converting VChR1 to C1V1, a functional redshifted opsin with a much stronger photocurrent output.^[10] **Table 1** lists representative opsins with distinctive absorption spectra that are currently being investigated.^[3,8–10,13b,18–20]

It is noteworthy that all the opsins described above are suitable for only neuronal activation. The inhibition of neuronal activity can be accomplished using Cl[−]-transporting

Table 1. List of commonly used opsins.

Opsins	Absorption wavelength [nm]	Mode	Remark
ChR1 ^[18]	500	Activation	Derived from <i>Chlamydomonas reinhardtii</i> ; slower desensitization than ChR2.
ChR2 ^[3,18a]	460	Activation	Derived from <i>Chlamydomonas reinhardtii</i> ; enables temporal control of neuronal activity on the millisecond scale but at the risk of a high level of desensitization; good expression level on membranes; commonly used for optogenetics.
VChR1 ^[9,10]	589	Activation	Derived from <i>Volvox carteri</i> ; redshifted opsin with a similar photocurrent as ChR1; low efficiency in high frequency stimulations due to slower photocurrent kinetics; poor level of membrane expression; challenging for in vivo applications.
C1V1 ^[13b]	549	Activation	A chimeric combination of ChR1 and VChR2; inferior to ReaChR in membrane trafficking and opsin expression; can be targeted by green-emitting UCNPs.
ReaChR ^[8]	590–655	Activation	Activatable by an excitation even at 655 nm in vivo; slower channel closing rate than other common opsins; better membrane trafficking and opsin expression than VChR1.
C128A, C128S ^[20]	Activation—470 Deactivation—(≈560)	Activation (Step-function/bi-stable)	Applicable to low intensity irradiation; amenable to an increased channel closing rate with longwave irradiation; C128S is useful for low intensity activation but lacks temporal precision, whereas C128A is more applicable to rapid activation and deactivation.
NpHR ^[19]	525–650	Inhibition	Derived from <i>Natronomonas pharaonis</i> ; light-driven chloride pump for hyperpolarizing neurons; inhibition of action potential firing at moderate membrane expression levels; poor trafficking to the membrane; can be coupled with ChR2 to provide neuronal activation and inhibition.
eNpHR & variants ^[21b]	593	Inhibition	Derived from <i>Natronomonas pharaonis</i> ; developed to overcome the problems associated with NpHR membrane trafficking; safe, high-level expression with augmented inhibitory function; increased peak photocurrent in the absence of aggregation.
Arch 3, Arch T ^[21a]	540–589	Inhibition	Derived from <i>Halorubrum sodomense</i> (Arch 3) and strain TP009 (Arch T); Arch 3 was discovered as a light-driven outward proton pump that is suitable for repeated cycles and chronic inhibition of neuronal activity; Arch T is the improved version of Arch 3 with higher light sensitivity, photocurrents and expression levels.

halorhodopsins (NpHR), which hyperpolarize the membrane potential of the neuron and inhibit the generation of action potential and firing of neurons.^[19] Further improvement was made to enhance the expression level at the membranes of neuronal cells. Optogenetic actuators based on proton-pump rhodopsins, such as archaerhodopsin 3 (ArchT) from the *Halorubrum* strain TP009 and enhanced bacteriorhodopsin derived from *Natronomonas pharaonic*, have also been studied as inhibitory optogenetic actuators.^[21]

Step function opsins are another type of specialized optogenetic actuators that are highly sensitive to low-intensity-excitation light. After a pulse of light stimulation, step-function opsins keep their channel pores open for an extended period, permitting a continuous transmembrane ion flux. A short pulse of light at a longer wavelength conveniently shuts down step-function opsins.^[10,20] The bistable nature of the step-function opsins also implicates the protein channel's ultrasensitivity to light stimulation. The light intensity required to activate step-function opsins can be orders of magnitude lower than that used for wild-type ChR experiments.^[20]

Owing to their robustness and malleable features, optogenetic methods have found numerous applications in elucidating neural and signal transduction pathways. For instance, they have been used to map the barrel cortex representation of whisker follicles in rodents^[22] and to regulate the medial frontal cortex to elicit antidepressant effects.^[23] In the spinal cord, the application of optogenetic methods has helped identify various subgroups of neural networks that regulate the movement of limbs.^[24] Proper optogenetic stimulation of targeted neural pathways in the spinal cord has even conferred functional recovery of breathing in damaged spinal circuits.^[25] Furthermore, the neuromodulation of pain receptors has been coupled with optogenetics to stimulate nociceptive neurons.^[15a,26] On non-neural cells, modulation by optogenetics has been used to regulate skeletal muscle,^[27] heart muscle,^[28] and insulin production.^[29] The first clinical trial using optogenetics to replace lost neurons in retinitis pigmentosa neurodegeneration has also been reported.^[30] Retinal ganglion cells were induced to be light sensitive by optogenetics in the hope of replacing degenerated photoreceptors. In addition to the dissection of neural functions in sensation, cognition, and action, optogenetic methods have also shed light on neurological disorders. Neural circuits related to seizure,^[31] Parkinson's disease,^[32] Alzheimer's disease,^[33] and drug addiction^[34] have been intensively investigated using optogenetic tools. The fresh insights gained from recent optogenetic experimentation should lay the groundwork for future development of pharmaceutical treatments that target disorders of the central nervous system (CNS).

2.2. Light-Delivery Challenges in Optogenetics

Despite the encouraging advancements in optogenetic techniques, the critically low penetration of visible light limits their in vivo applications. For in vivo optogenetic studies, one must consider how to deliver light effectively and noninvasively through tissues. Visible light of notably short wavelength attenuates significantly along its optical path through tissues due to scattering and absorption. It is estimated that, in mammalian

brain tissues 0.5 mm distal from the optical fiber, only 10% of the initial visible-light power density remains.^[35] Considering that the scalp and skull of a rodent typically have a combined thickness of approximately 1.3–1.8 mm,^[36] it is highly unlikely that visible light can be used to directly activate neurons with non-contact external-illumination methods. A standard setting for in vivo light delivery uses a cannula-based fiber-optic that is surgically implanted in the brain.^[17a] However, this fiber-optic insertion method is not without its own limitations and complications. Prolonged high-frequency optogenetic stimulation also generates heat and may cause phototoxicity. Depending on the exact location of the neuron population under investigation, the fiber-optic tip is typically installed just through a 300 μm (in mice) and 1 mm (in rats) thickness of their skull.^[5] Deeplying neurons are therefore inaccessible to light stimulation even with fiber-optic insertion. Additionally, due to the invasiveness of such a method, tissue damage, injection site infection, and inflammation may occur without proper precautions. The movement of the animal may cause displacement of the inserted fiber-optic tip, which would not only lead to off-target light delivery but also cause additional damage to the brain tissue. Furthermore, the fiber light source and the associated electronics are head mounted or tethered to the head using a commutator, which also significantly limits the range of motion in rodents, such as in the large radial or water mazes used in behavioral studies.^[6] These obstacles have been partially overcome by the advent of wireless and implantable optogenetic stimulators.^[35b,37] A recent design based on microscale optoelectronic implants allows NIR upconversion to take place directly on an array implanted into the brain.^[38] The encapsulation of the implants with biocompatible surfaces led to an enhanced local field potential for an in vivo optogenetic mice model upon excitation at 810 nm. In a miniaturized optoelectronic set-up, photovoltaic diodes were used to convert infrared photons and power LED emission.

The use of visible light in wireless stimulators is also subject to scattering by tissue and poor depth penetration. However, these problems can be addressed with NIR light because light absorption and light scattering are highly wavelength dependent. For light scattering, the intensity of the scattered light is proportional to $1/\lambda^4$. Therefore, NIR light has a strong tendency to travel with less scattering in media such as the brain and be efficiently delivered to targeted neurons. In addition, compared to visible light, NIR light is absorbed minimally by hemoglobin in the blood and melanin in the skin. Although water can absorb NIR irradiation at certain wavelengths, several optical windows in the NIR spectrum allow good light penetration through tissues, as there is less water-associated absorption in these optical windows. In addition, these NIR optical windows (NIR-I window: 650–950 nm; NIR-II window: 1000–1350 nm) have been extensively utilized for photoluminescence-based deep-tissue imaging experiments.^[39]

Hence, if neurons can be activated by NIR-light irradiation, in vivo deep-tissue optogenetic studies should not be restricted by LEDs, optical fibers, and tethering. Even though NIR-light-responsive opsins have yet to be discovered, it is possible to circumvent the technological challenges by employing materials that convert NIR irradiation into visible-light emission through the upconversion process.^[40]

3. Upconversion Materials

To achieve photon upconversion, the luminescence center has to absorb multiple photons and subsequently emit a single photon in one excitation–relaxation cycle. Although it may sound counterintuitive to convert lower energy photons into higher energy photons via luminescence, selective elements in the lanthanide series are particularly good for this upconversion purpose.^[41]

3.1. Upconversion Mechanisms

Trivalent lanthanide ions such as Ho^{3+} , Er^{3+} , and Tm^{3+} have ladder-like energy levels. The similar spacing between neighboring energy levels permits the population of the higher energy levels through sequential absorption of multiple incoming photons. This sequential energy-pumping mechanism for lanthanide elements is in stark contrast with the two-photon absorption process, which strictly requires the simultaneous absorption of two photons in a single luminescence center. Consequently, the excitation power threshold for realizing upconversion in lanthanide elements is orders of magnitude lower than that required for two-photon absorption, and a high-peak-power femtosecond laser and focal lens is not needed when working with lanthanide-based upconversion materials.

Depending on the material construct and energy-level-population pathways, upconversion processes can be classified into four categories: excited-state absorption upconversion, energy transfer upconversion, cooperative sensitization upconversion, and photon avalanche.^[40a] Among them, energy-transfer upconversion provides the highest upconversion efficiency. In typical energy-transfer upconversion, Yb^{3+} ions in the inorganic host crystals act as sensitizers that absorb NIR photons. The excited Yb^{3+} ions can subsequently transfer their energy to neighboring emitter ions such as Er^{3+} and Tm^{3+} . By receiving multiple energy quanta from the sensitizers, the emitters can be successively promoted to higher energy levels, which subsequently leads to upconversion luminescence.

3.2. Excitation Wavelength Tuning of Upconversion Materials

Since Yb^{3+} ions have absorption peaks centered at 980 nm, continuous-wave lasers of this wavelength are commonly used as the excitation source for performing upconversion in lanthanide-based materials. However, water absorbs light strongly in this wavelength range, which raises a concern for tissue overheating under poorly controlled NIR exposure. Recently, efficient upconversion with 745 and 800 nm excitation has been achieved by introducing Nd^{3+} as a sensitizer into the conversion material.^[42] Because the absorption coefficient of water is ten times lower at 745 and 800 nm than at 980 nm, using 745 and 800 nm light to trigger the upconversion process can be more efficient, reducing the light-intensity/energy requirements and thus greatly mitigating the overheating side effect caused by NIR irradiation. A convenient feature of upconversion emission is that the emission color output can be readily controlled and

that the emission color is barely affected by the excitation wavelength. Therefore, regardless of which excitation wavelength is chosen for an optogenetic experiment, blue, green, yellow, and red emission can always be achieved as required. Thus, the upconversion approach affords dual benefits: the delivery of light in the NIR range and the emission of desirable blue, green, or yellow light for optogenetic stimulation.

3.3. Emission-Color Modulation of Upconversion Materials

Controlling the color output of upconversion emission is an essential part of accomplishing NIR-optogenetic-induced neuronal activities. The absorption bands of several kinds of opsins fall into different spectral regions. Neuron activation with maximum efficiency is optimum if the upconversion emission peak is tuned to match the absorption spectrum of the opsin under investigation.

The $f-f$ electronic transitions between discrete lanthanide energy levels result in narrow upconversion emission peaks (full width at half maximum of ≈ 30 nm) at fixed wavelengths, and the emission wavelength is highly dependent on the lanthanide emitter identities. For example, the Tm^{3+} emissions at 450 and 475 nm are suitable for activating ChR2, whose absorption lies in the blue spectrum. Furthermore, Er^{3+} ions have characteristic upconversion emission peaks located at 409, 525, 546, and 659 nm, and the peaks at 525 and 546 nm are favorable for activating VChR1 and C1V1 opsins, respectively (Figure 2).^[43]

For experiments that only involve opsins responsive to a broad activation spectrum, the presence of redundant emission peaks at 409 and 659 nm is not a concern. However, if single-wavelength emission is required for a particular optogenetic experiment, the redundant emission peaks must be suppressed to avoid the unwanted photoactivation of opsins. Fortunately, several methods have been developed for upconversion color tuning. For instance, decreasing the Yb^{3+} doping concentration in a host crystal significantly suppresses the 659 nm emission peak, resulting in purely green emission.^[44] In contrast, if Mn^{2+} ions are co-doped with Yb^{3+} and Er^{3+} , the emission peaks at 525 and 546 nm can be completely diminished, resulting in a predominantly red output.^[45] Apart from the use of ion doping to manipulate emission spectrum profiles, it is also feasible to adopt nanosized color filters to obtain monochromatic emission from upconversion materials.^[46]

Although emissions from common upconversion emitters such as Ho^{3+} , Tm^{3+} , and Er^{3+} already cover a broad spectral range, their emission does not extend over the yellow band ranging from 550 to 650 nm, which can be used to control Cl^- -pumping halorhodopsins. Recently, two methods were reported to have achieved unprecedented Eu^{3+} upconversion emission at 590 and 616 nm through either energy-migration upconversion^[47] or cooperative-sensitization upconversion.^[48] The dual emission peaks at 590 and 616 nm match well with the absorption spectra of halorhodopsins and therefore can serve as neuron silencing signals. Alternatively, methods relying on Förster resonance energy transfer (FRET) can make upconversion materials emit yellow light. Li et al. demonstrated that coating the surface of the upconversion material with fluorophores such as tetramethylrhodamine isothiocyanate (TRITC) allows TRITC to accept energy from Er^{3+} donors through FRET,

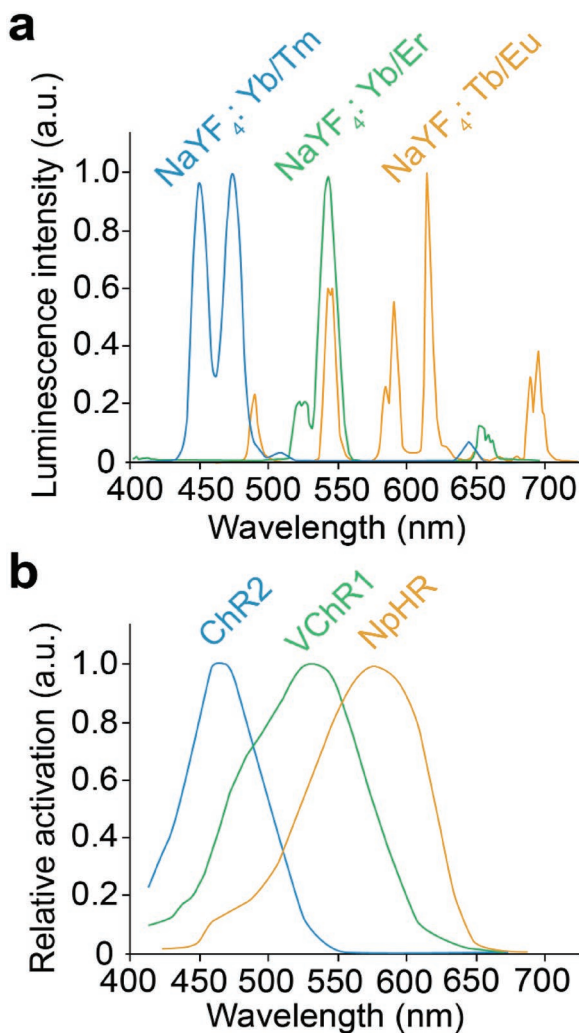


Figure 2. a) Luminescence spectra of selected UCNPs with emission peaks overlapping with the absorption wavelengths of commonly used opsins. Blue curve: NaYF₄ host doped with 30% Yb³⁺ and 0.5% Tm³⁺. Green curve: NaYF₄ host doped with 5% Yb³⁺ and 1% Er³⁺. Yellow curve: NaYbF₄:Tb@NaTbF₄@NaYF₄:Eu core-shell-shell nanoparticles. b) Absorption spectra of commonly used opsins. a,b) Reproduced with permission.^[5] Copyright 2010, Springer Nature.

resulting in a broad emission band in the 570–630 nm wavelength range.^[49] Overall, it can be concluded that by rational tuning of the color output of the upconversion emission, most of the opsins discovered thus far can, in principle, be successfully activated by lanthanide-based upconversion emission.

The coexpression of ChR and halorhodopsins allows the convenient activation or inhibition of neurons with blue and orange light, respectively.^[19] Such an application requires at least two light sources to selectively regulate neuronal electrophysiological activities. Fortunately, this requirement for color-output switching can also be met using a single upconversion nanoparticle. In recent work, Lai et al. constructed a multilayer nanoparticle that emits different colors when the excitation is switched between 800 nm and 980 nm excitation.^[50] The creation of such UCNPs with orthogonal emission characteristics implies that in the future, two populations of

deep-lying neurons will be able to be independently controlled by the application of NIR irradiation at two wavelengths.

3.4. Enhancing the Upconversion Emission Brightness

In addition to resulting in good spectral overlap between the upconversion emission and opsin absorption, realizing strong upconversion emission intensity is equally important for NIR-based optogenetic experiments.^[51] A neuron evokes an action potential in an all-or-none fashion through which the light-induced depolarization needs to surpass the threshold potential (≈ 55 mV) from its resting membrane potential (≈ 70 mV). Consequently, upconversion emission would have to drive sufficient opsin activation to exceed this threshold.

The most effective approach for enhancing upconversion emission involves the application of higher excitation powers. Due to multiphoton absorption, the upconversion emission intensity follows a nonlinear relationship with the excitation power.^[52] Increasing the power of the excitation source generally results in a much faster growth in the emission intensity. However, in the context of bioapplications, unregulated light and material exposure compromises the living status of neurons due to laser-light-induced overheating and potential nanoparticle toxicity. Therefore, additional efforts should be made to increase the brightness of each individual particle under a fixed excitation power.

The brightness of any given luminescent material is governed by its light-absorption coefficient and luminescence quantum yield. The light-absorption coefficients of trivalent lanthanide ions are intrinsically low due to the parity-forbidden nature of the *f-f* electronic transition. Since a large portion of the incoming photons are not utilized for generating upconversion emission, the emission intensity is generally too weak to be observed under incoherent light excitation. NIR dyes have been applied to assist the energy-harvesting process for lanthanide ions to overcome the restraints imposed by weak lanthanide absorption.^[53] Organic-based NIR dyes have absorption coefficients that are three to four orders of magnitude higher than those of lanthanide ions. When NIR dyes are attached to the surface of the upconversion material, they can act as “antennas” in harvesting NIR irradiation and subsequently transferring the absorbed energy to lanthanide ions for further upconversion. Using the dye-sensitization strategy, the upconversion emission intensity is fourteen times greater than that of dye-free upconversion materials, and the developed materials can even generate visually observable upconversion emission under incoherent light excitation (Figure 3).

In addition to the light-absorption coefficient, the luminescence quantum yield, defined as the ratio of the number of emitted photons to the number of absorbed photons, is equally important in determining the brightness of luminescent materials. Several methods, including choosing host materials with a low phonon energy,^[54] breaking the host crystal’s symmetry,^[47,55] and controlling the lanthanide doping concentration,^[56] have also been discovered to improve the quantum yield of upconversion materials. Among these methods, surface passivation has proven to be one of the most effective (Figure 3).^[57]

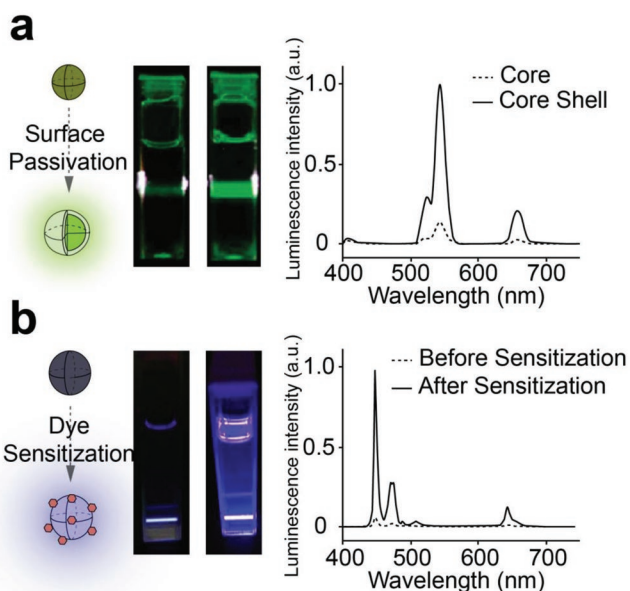


Figure 3. Two common strategies for enhancing the upconversion emission intensity. a) Surface passivation on upconversion particles to suppress surface quenching, which leads to an eightfold enhancement in the Er^{3+} emission at 550 nm. Reproduced with permission.^[57a] Copyright 2007, ACS Publications. b) The dye-sensitization strategy to increase the light harvesting capability of upconversion materials, which results in a 14-fold enhancement in Tm^{3+} emissions at 450 and 475 nm. Reproduced with permission.^[57b] Copyright 2015, ACS Publications.

In the surface-passivation method, upconversion crystals are coated with an optically inert shell material through an epitaxial growth mechanism.^[58] The shell layers prevent direct contact between the Yb^{3+} and the C–H- and O–H-containing molecules because this contact causes luminescence quenching. This strategy is particularly helpful in improving the quantum yield for nanometer-sized upconversion materials because their enormous surface-area-to-volume ratio often results in significant surface quenching. Generally, a tenfold increase in the quantum yield can be anticipated after coating a 30 nm sized upconversion particle with a 5 nm shell layer. A power output study of these core–shell-structured nanoparticles suggests that, under an excitation power density of 0.5 W mm^{-2} , 0.1 mg of such nanoparticles generates 0.5 mW green-light emission, which is sufficient for triggering neuron firing. The power density is calculated by considering the area of a beam using the radius and dividing the beam's power by that area, which is expressed in units of W cm^{-2} or W mm^{-2} . However, for in vivo optogenetic studies, NIR light often experiences some intensity attenuation along the optical path. There is a pressing demand to develop stronger upconversion emitters to compensate for this loss in excitation power in in vivo optogenetic applications.

3.5. Upconversion Luminescence of Bulk to Nanosize Materials

The upconversion phenomenon was first studied in bulk crystals and glass materials decades ago.^[40a] However, to apply these wavelength-transducing materials to the field of

optogenetics, it is necessary to reduce their size to the sub-micrometer regime. This size range would render the delivery of these materials into living organisms much easier and less invasive. Fortunately, several methods, including hydrothermal synthesis,^[59] co-precipitation,^[60] and thermal decomposition,^[61] have been developed to synthesize monodispersed upconversion nanocrystals with a wide range of size options, from sub-10 nm to greater than $5 \mu\text{m}$. The as-synthesized particles are often only soluble in nonpolar solvents due to the hydrophobic ligands used in the synthesis. Additional surface modification is required to make them water soluble.^[62]

UCNPs without any surface ligand protection can interact with intracellular biomolecules and hence exhibit a certain level of toxicity.^[63] To prevent such unwanted interactions, biocompatible polymers are often coated to the nanoparticle surface to form an intact molecular sheath.^[64] Poly(ethylene glycol),^[65] owing to its excellent water dispersity and low toxicity, is often selected as the nanoparticle coating for in vivo luminescence imaging and photodynamic therapy experiments;^[66] however, in those applications, a portion of the administered UCNPs eventually localize in the liver and spleen. Physiological and histological assessments suggest that UCNPs with proper surface modification cause negligible side effects to living organisms during experiments.^[67]

Current research studies lack a unifying protocol for the toxicological profiling of UCNPs on neurons and the brain. Although extrinsic materials such as Fe_3O_4 ^[68] and microLEDs^[37b] have shown satisfactory biocompatibility after being implanted in the brain for neuron manipulation purposes, lanthanide-based upconversion particles, which are a different type of nanoparticle, may induce a certain level of toxicity to the nervous system due to their unique composition, morphology, and surface chemistry. In the in vivo optogenetic setting, UCNPs must be implanted as close as possible to opsin-expressing neurons. Additional systematic studies with a main focus on the CNS should be conducted to evaluate the neurotoxicity of nanoparticle implantation.

4. Case Studies of Existing NIR Optogenetic Systems

The concept of upconversion-enabled NIR optogenetics was first demonstrated at the cellular level using the whole-cell patch-clamp technique, in which a glass micropipette containing a silver electrode is used to record and amplify the current changes across the membrane. For the action potentials to be measured, the ionic current is kept constant by a compensatory current injection feedback system, and the changes in voltage are recorded.

Hososhima et al. cultured C1V1 and *Platymonas subcordiformis* (PsChR)-expressing cells on films containing UCNPs and performed whole-cell patch-clamp studies to demonstrate the feasibility of NIR-light-induced neuronal activity.^[13b] In their work, hydrothermally synthesized upconversion crystals measuring $100 \text{ nm} \times 500 \text{ nm}$ in size were mixed with collagen to form a neuron culture substrate. When an NIR laser was pointed at the specially designed substrate, upconversion emission illuminated the neurons from the bottom to induce neuronal responses. By implanting upconversion materials in

a biocompatible polymer support, the direct contact between the lanthanide ions and neurons can be avoided and thus particle-induced cytotoxicity is not a concern.

Their experimental results showed that the irradiation of a green-emitting upconversion substrate with a 980 nm laser resulted in C1V1-expressing neurons producing inward photocurrents and that the laser irradiation also evoked action potentials. The photocurrent was also observed in PsChR-expressing cells if a blue-emitting upconversion material was chosen to form the upconversion film. Nonetheless, the developed method requires a relatively high NIR excitation source power of $\approx 58 \text{ W mm}^{-2}$. In comparison, 14 mW mm^{-2} green illumination is sufficient to generate an even higher photocurrent under the same setup.^[13b] Based on this comparison, it is estimated that the energy-transfer efficiency of upconversion materials is less than 0.024%. The authors also noted that under such high-power excitation, neurons experience small-magnitude photocurrents, even in the absence of upconversion materials.^[13b] These trace photocurrents are likely due to the temperature increase sensed by the naturally present temperature-sensitive transient receptor potential (TRP) channels. Therefore, for in vivo applications, overheating caused by continuous laser irradiation must be suppressed to avoid excessive noise action potentials.

Shah et al. conducted a similar patch-clamp study (Figure 4).^[69] In their approach, they mixed core-shell UCNPs and poly(lactic-co-glycolic acid) to form the upconversion substrate and investigated the NIR response of ChR2-expressing neurons. Because core-shell UCNPs exhibit a higher quantum yield than nonpassivated upconversion crystals, their blue emission provides enough power to depolarize ChR2-expressing neurons. As a result, high-temporal-resolution neuron responses were achieved in this work. Repetitive action potentials were observed at frequencies up to 10 Hz under pulsed NIR-light irradiation. In the same study, the authors also conducted optogenetic tests on UCNPs without shell passivation. They found that the shell-lacking nanoparticles resulted in inconsistent and unreliable nerve impulse generation and required higher laser powers and longer laser-pulse durations to trigger neuron firing than their core-shell counterparts. This comparative study further confirmed that high quantum yield core-shell UCNPs are more suitable candidates for NIR-light-induced neuron activation.

In another study, Wu et al. observed neuron firing with NIR dye-sensitized upconversion illumination.^[70] According to the authors, dye-conjugated core-shell UCNPs exhibit seven times stronger emission than dye-free particles due to the “antenna” effect as described previously. An NIR laser power density of 1.5 W mm^{-2} was reported to be sufficient to generate an action potential; this power is the lowest of all patch-clamp studies.

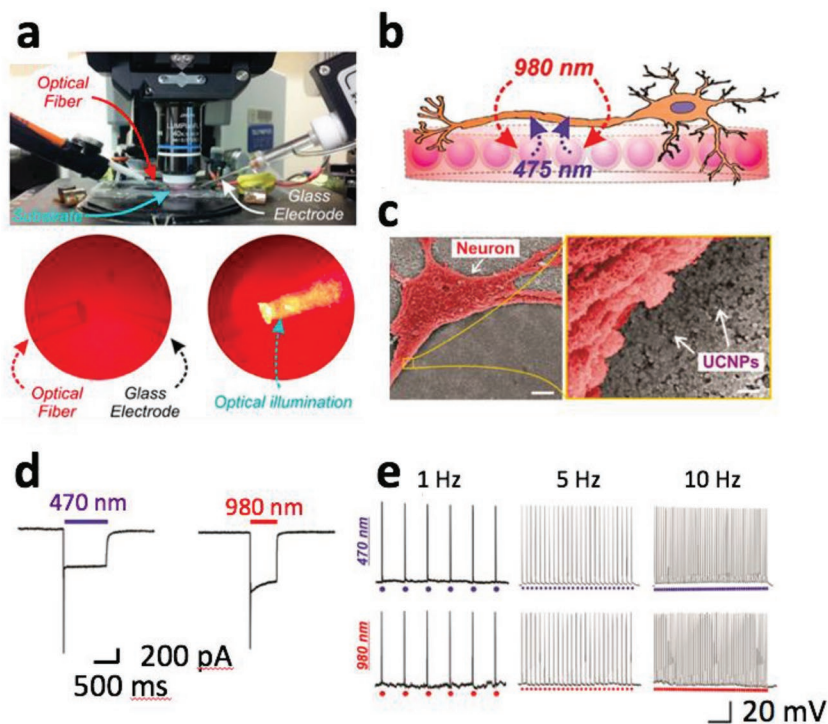


Figure 4. In vitro demonstration of NIR light-enabled optogenetics. a) Experimental setup for the patch-clamp study. NIR irradiation is guided to excite neurons through an optical fiber. Meanwhile, the glass electrode is patch-clamped to neurons to measure the current flow and voltage changes across the membrane. b) Scheme of nanoparticle–polymer thin film substrate for neuron incubation. c) Illustration of NIR-mediated optogenetics on neurons cultured onto the upconversion film. d) The inward current flow is measured after a brief 980 nm excitation. The current response is very similar to blue-light excitation. e) Bursts of action potentials were fired following 3 ms pulse light irradiation at either 470 or 980 nm. The neuron firing synchronizes with the light spiking pace even at a high frequency of 10 Hz. a–e) Reproduced with permission.^[69] Copyright 2015, Royal Society of Chemistry.

Nevertheless, it should be pointed out that many variables differ between the studies. For example, the opsin type used in their studies was a redshifted channelrhodopsin, and the upconversion nanoparticle concentration in the polymer film and the laser pulse duration affected the final performance of the patch-clamp experiments. These factors make direct comparison between different studies difficult. Considering that NIR dyes may undergo photobleaching and cause heat generation during continuous laser irradiation, whether dye-sensitized UCNPs outperform ordinary core-shell nanoparticles, especially in long-term optogenetic studies, is unclear.

The abovementioned studies employ the polymer thin film setup to prove the concept that NIR-induced upconversion emission can evoke neuronal activity. However, such setups are not feasible for in vivo studies due to several reasons. First, it would be technically challenging to implant the macroscopic polymer scaffold in the tight and deep extracellular space in the brain. Instead, the direct injection of tiny volumes of nanoparticles or particle-tagged cells appears to be more practical. Second, one must also consider the toxicity effects of extraneous nanoparticles when they interact with neurons. Although the side effects caused by lanthanide exposure can be alleviated by reducing the upconversion administration dosage, higher

NIR excitation powers are needed to compensate for the loss of emission centers. Consequently, laser-induced overheating may occur. Finally, for noninvasive *in vivo* neuron manipulation, light has to penetrate through fur, skin, skull, and layers of brain tissue. One cannot assume that NIR irradiation retains most of its initial power after tissue penetration. Therefore, although the *in vitro* patch-clamp technique is a straightforward way of characterizing neuron activity, *in vivo* NIR optogenetic experiments are necessary to prove that remote and noninvasive NIR-light-mediated neuronal control is possible.

Caenorhabditis elegans, a worm with a small nervous system of 302 neurons, is regarded as a simple but relevant *in vivo* model to investigate the causal relationship between neuronal activities and behavior.^[71] In a study reported by Zhang and co-workers,^[72a] by feeding UCNP to *C. elegans* with ChR2-expressing mechanosensory neurons, they found that the blue emission caused by NIR excitation drastically alters the *C. elegans* movement direction similar to applying a touch force to the worm (Figure 5a). In addition, by optimizing the upconversion feeding dosage and employing a quasi-continuous-wave laser at a low average power density, *in vivo* behavior control can be achieved with NIR light without causing overheating and particle-toxicity-related side effects on *C. elegans*. Note that, since *C. elegans* is an optically transparent organism, blue light can easily be used to manipulate its behavior. In another study, Xing and co-workers^[72b] selected the zebrafish as an *in vivo* model for optogenetic manipulation due to its physiological and genetic homology with mammals. The ion-channel of ChR2- and Ca²⁺-mediated biological functions can be remotely activated using 808 nm laser excitable UCNP (Figure 5b).

Lin et al. demonstrated the feasibility of using UCNP for the optogenetic modulation of targeted neural circuits in the visual cortex of rodents in a proof-of-concept study.^[73] In their study, NaYF₄-based nanoparticles with emission peaks at 470 nm

(Tm³⁺-doped) and 540 nm (Er³⁺-doped) were synthesized to activate ChR2 and C1V1 opsins, respectively. The biocompatibility of the UCNP was increased by loading and sealing dry nanoparticles in a glass micropipette (micro-optrode), which enabled their placement in close proximity to neurons without any direct contact with the cells. NIR pulses (980 nm) were applied to the tips of the optrodes to induce the emission of blue or green light. Electrophysiological recordings demonstrated the triggering of photocurrents and action potentials in both ChR2- and C1V-transfected neurons. Their study also provided preliminary *in vivo* evidence from the results of transfecting the visual cortex of adult rats with ChR2 and C1V1 genes and implanting doped nanoparticles at the virus injection sites. *In vivo* electrophysiological assessments verified the activation of the cortical neurons in anesthetized animals' post-NIR illumination.

Recently, Wang et al. provided the first evidence of upconversion-mediated, wireless manipulation of neural circuitry in awake, freely moving animals (Figure 6).^[74] Using the same optrodes described above, they implanted UCNP in three locations in the brain: the ventral tegmental area (≈4.5 mm deep), the cortical striatum (≈3 mm deep), and the visual cortex (≈1 mm deep). The microdevice optrode was ≈100 μm in diameter and less than 1 mg in weight, which renders it suitable for brain implantation without extensively damaging the tissue integrity of the brain. Efficient NIR illumination was ensured for a freely moving animal by the design of a robotic laser projection system capable of automatically locating the animal's head. Significantly, their results indicate that UCNP can be used for transcranial and deep-brain stimulation for behavioral conditioning, locomotion pattern modulation, and reflexive learning in awake, freely moving rodents. These studies also addressed several key concerns of applying upconversion technology in a biological system by providing evidence for a lack of a significant increase in inflammatory responses after the

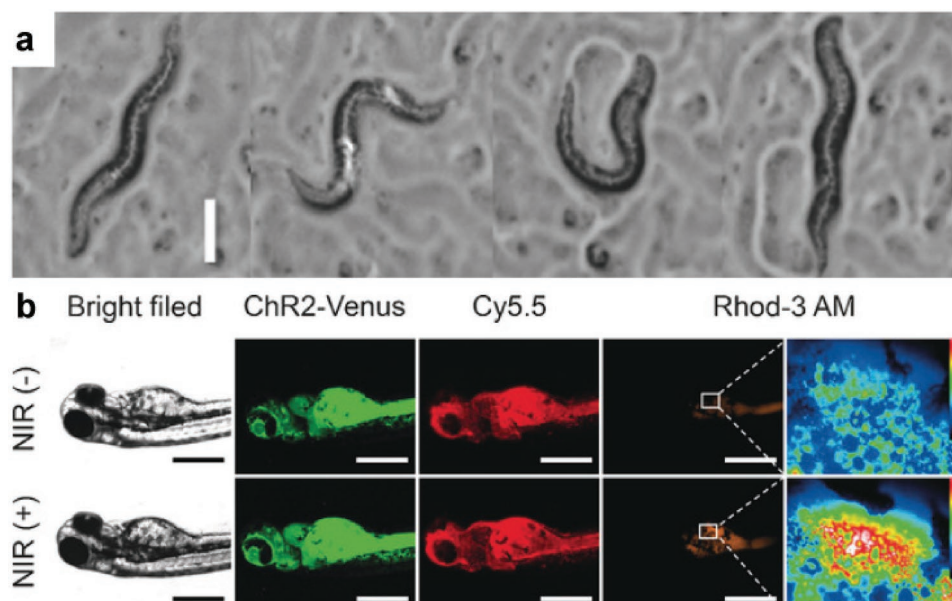


Figure 5. Optogenetics in *C. elegans* and zebrafish models. a) Representative images showing a reversal process of a worm expressing ChR2 with treatment of UCNP under NIR irradiation. Reproduced with permission.^[72a] Copyright 2016, Wiley-VCH. b) Fluorescence imaging with and without NIR treatment in zebrafish incubated with DBCO/Cy5.5-UCNP. a, b) Reproduced with permission.^[72b] Copyright 2017, Wiley-VCH.

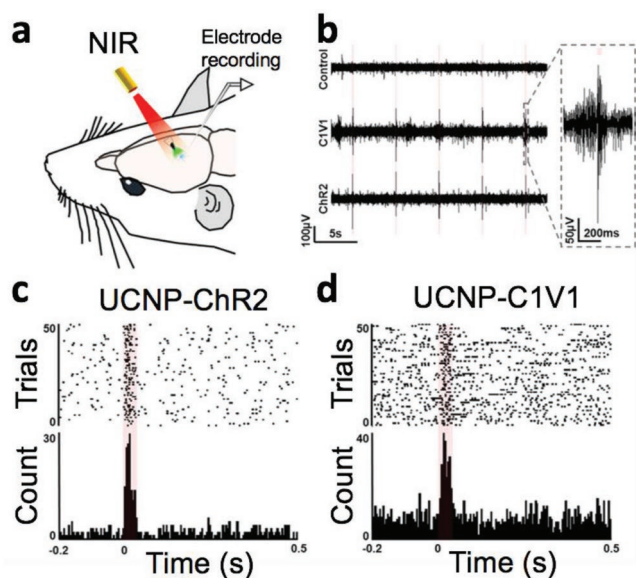


Figure 6. In vivo NIR upconversion-based optogenetics. a) Schematic of the experimental setup. An upconversion-nanoparticle-containing microdevice was implanted into a mouse brain. Neuron activities were controlled through pulsed NIR excitation and recorded with implanted electrodes. b) Recordings of NIR-driven spiking traces in neurons expressing either C1V1 or ChR2. c, d) Raster plots and peri-stimulus time histograms showing neuronal responses under one brief pulse of NIR irradiation. a, b) Reproduced with permission.^[74] Copyright 2017, Elsevier.

implantation of an upconversion microdevice. Additionally, they reported no changes in skin temperature upon NIR illumination and no heating effect due to the upconversion emission.

In another recent study by Chen et al.,^[75] core-shell-structured UCNPs were injected in the hippocampus of

mice, where neurons encoding fear memory expressed ChR2 (Figure 7). The transcranial NIR-light irradiation (without insertion of any kind of optical fiber) induced the freezing behavior of the freely movable mice. This was a clear indication of recalling the fear memory even two weeks after injection of UCNPs. In these studies, there were no signs of tissue damage, inflammation, or apoptosis. This approach was further validated with various modalities of neuronal control, including the inhibition of neural circuitry and the entrainment of hippocampal theta oscillation. The results also demonstrated the long-term stability of UCNPs and low dispersion in nervous tissue. The nanoparticles remained localized in and around the site of implantation in the brain even after one month with minimal signs of cytotoxicity and immune response. The anesthetized mice were exposed to transcranial pulsed NIR irradiation (15 ms pulses at 20 Hz, 3 s every 3 min for 30 min, 3.0 W peak power, 15 mW average power, 1.4 W mm⁻² power density), the irradiation did not cause any damage in tissues during in vivo experimental procedures. It is noteworthy that the fur was removed, and an incision was made in the skin above the intact skull without undergoing skull-thinning, skull-opening or any other treatment for in vivo experimental procedures. The report clearly suggests that there are no major complications due to small temperature rise. These results suggest that the precise control of multimodal deep brain neuromodulation in rodents can be achieved with transcranial NIR excitations.

Recently, Miyazaki et al. in 2019 reported the use of upconversion optogenetics for freely movable animals.^[76] They developed minimally invasive “fiberless” optogenetics using lanthanide microparticles. These microparticles emit visible light in response to NIR illumination. The researchers reported depolarizing (or activating) C1V1 and hyperpolarizing (or inhibiting) ACR1 opsins. This semi-invasive technique enabled them to manipulate motor behavior of freely behaving mice by

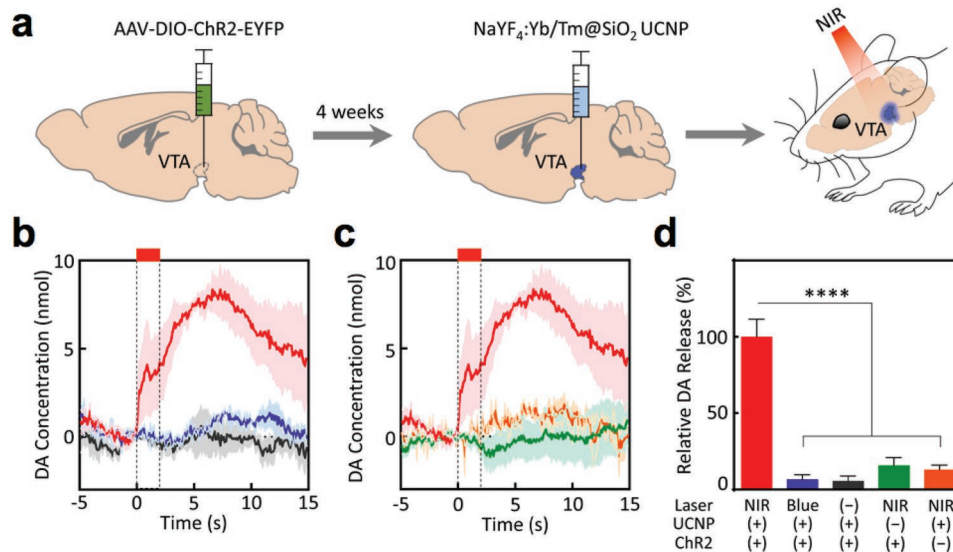


Figure 7. NIR deep-brain stimulation through upconversion-nanoparticle-mediated optogenetics. a) In vivo experimental scheme for transcranial NIR stimulation of the ventral tegmental area (VTA) in anesthetized mice. b, c) Transient dopamine concentrations in the ventral striatum in response to transcranial VTA stimulation under different conditions. Each color corresponds to a condition shown in (d). d) Cumulative dopamine release within 15 s after the start of transcranial stimulation under the five conditions presented in (b) and (c). a–d) Reproduced with permission.^[75] Copyright 2018, American Association for the Advancement of Science.

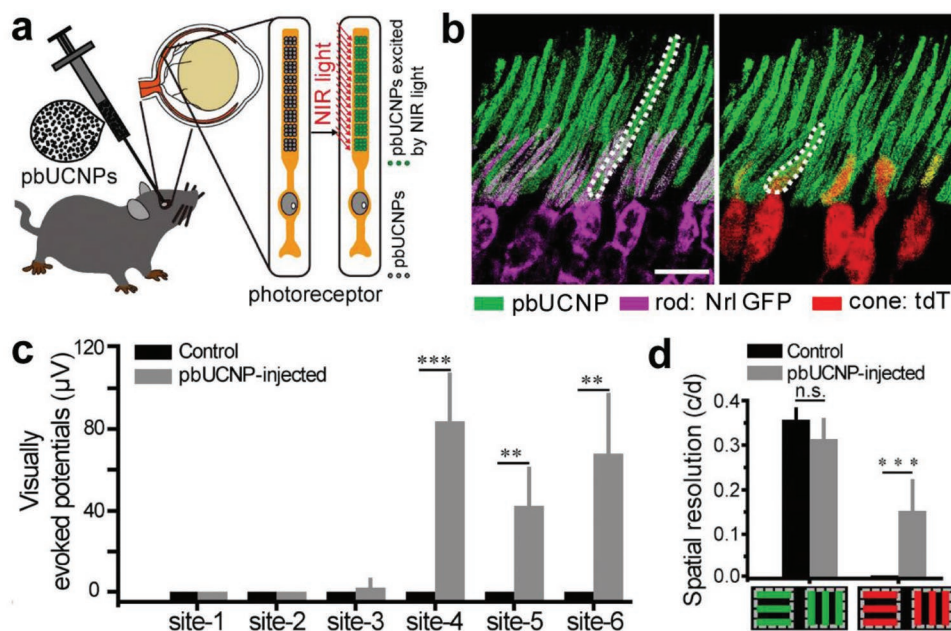


Figure 8. Mammalian near-infrared vision through UCNP-mediated optogenetics. a) Illustration of subretinal injection of photoreceptor-binding UCNPs (pbUCNPs) in mice. b) Merged fluorescence images of retina from pbUCNP-injected mice. The dashed lines show a continuous inner and outer segment of a rod and a cone. Scale bar, 10 mm. c) Peak of visually evoked potentials triggered by 980 nm light at each recording site. d) Visual spatial resolutions of pbUCNP-injected and control mice for 535 nm (green pattern) and 980 nm (red pattern) light gratings. a–d) Reproduced with permission.^[77] Copyright 2019, Elsevier.

activating and inhibiting selective neurons expressing C1V1 and ACR1 in the dorsal striatum, respectively.

In 2019, Ma et al.^[77] reported that NIR image vision can be enabled through sub-retinal injection of photoreceptor-binding UCNPs (Figure 8). This was the first demonstration based on implantable optical nanomaterials for extending the scope of their application to night vision in an animal model. The adverse effect to retina was negligible even two months after injection of UCNPs. A relatively low intensity (1.62 mW cm^{-2}) from an NIR LED was adequate to allow the animals to see light beyond the visible spectrum. For better comparing in vivo optogenetics using UCNPs in rodent models, we summarized total power and the average laser intensity of NIR irradiation and their applications in Table 2.^[73–79]

The applications of upconversion technology in biological systems are not limited to neuroscience research because genetically encoded “photoswitches” can be expressed in other types of cells to enable the light manipulation of cellular functions.^[80] In 2015, He et al. demonstrated the feasibility of in vivo NIR optogenetic control of subcutaneous cellular immune responses.^[78] In this work, the Ca^{2+} -release-activated Ca^{2+} (CRAC) channel was made photosensitive by protein-engineering methods. Consequently, blue light can be used to trigger Ca^{2+} influx in engineered T-cell hosts, which leads to further cell immune responses. To demonstrate that NIR irradiation can cause Ca^{2+} influx beneath the skin, core-shell UCNPs were first attached to cells using the streptavidin

tag. Subsequently, the particle-tagged cells were implanted subcutaneously in the flanks of mice. Upon NIR-light irradiation, Ca^{2+} flow and downstream protein expression were successfully visualized by luciferase-catalyzed bioluminescence. Furthermore, the authors incorporated this NIR-mediated immunomodulatory concept into tumor therapy by demonstrating that NIR stimulation helped dendritic cell maturation and consequently suppressed tumor growth. In addition, the thermal imaging indicated nonsignificant increase in temperature, although a relatively high power density of 30 mW mm^{-2} of 980 nm laser was used, which is higher than the norm in skin exposure (3.6 mW mm^{-2} under ANSI Z136.1–2007 Orlando FL Laser Institute of America 2000). Several factors contributed to

Table 2. List of animal type and average laser intensity in the current upconversion optogenetic studies.

Ref.	Animal	Power	Application
[73]	Rat	$1.7\text{--}7.1 \text{ mW mm}^{-2}$	ChR2/C1V1 protein stimulation
[74]	Mouse/rat	$1.5\text{--}7 \text{ mW mm}^{-2}$	Remote control of neural activity in brains
[75]	Mouse	1.4 W mm^{-2} $15 \text{ mW average power}$	Deep brain stimulation
		2.1 W mm^{-2} $22.5 \text{ mW average power}$	Neural activity inhibition
[76]	Mouse	0.2 mW mm^{-2} 18.6 mW mm^{-2}	Neural activity activation Neural activity inhibition
[77]	Mouse	1.62 mW cm^{-2}	Mammalian near-infrared image vision
[78]	Mouse	30 mW mm^{-2}	Optogenetic modulation of immunoinflammatory responses
[79]	Mouse/rat	$0\text{--}6 \text{ mW mm}^{-2}$	Wireless optogenetic inhibition

the success of this NIR-mediated deep-tissue cellular response study. First, by taking advantage of streptavidin–peptide interactions, the authors brought UCNPs into close proximity to ion channels, which favors upconversion-emission harvesting by the Ca^{2+} channel. Second, the newly engineered ion channel appears to be intrinsically sensitive to light irradiation. It was reported that $40 \mu\text{W mm}^{-2}$ 470 nm (blue light) irradiation or 30 mW mm^{-2} 980 nm (NIR) irradiation can trigger the Ca^{2+} influx. This power requirement is much lower than that for conventional optogenetics. As a result, despite the light attenuation in the *in vivo* experiments, the light eventually reached the cells with ample intensity to evoke cellular responses. Based on this penetration, we envision that if highly light-sensitive step-function opsins are used in optogenetic experiments, remote NIR neuronal manipulation can be achieved in the rodent brain.

It is noteworthy that there are already reports on the testing of certain intra-parenchymal implantable and miniaturized wireless optogenetic devices in freely movable animals.^[81,82] However, UCNP-based intervention holds a unique advantage of being semi-invasive with low risk of infection for *in vivo* neuromodulation. By developing a minimally invasive method to stimulate selective neuro pathways located within deeper structures of the nervous system, the intention has been focused on using a non-electrical, non-electromagnetic, and non-electrode-based implantation approach to depolarize and hyperpolarize targeted neurons. This is feasible by replacing conventional approach to emit visible light by non-invasively exciting implanted UCNPs using near-infrared illumination approach and optimizing the visible-light emission of UCNPs within the parenchymal in order to activate light-sensitive ion channels in transfected neuro pathways.

Both commercially available wireless optogenetics technologies and newly developed nanoparticle applications in optogenetics have their own specific sets of advantages and disadvantages. As reported, one of the major differences is the invasiveness of the electrode-based implantation approach of wireless technologies versus the semi-invasive approach (one-time injection of nanoparticles). On the other hand, currently, UCNP-dependent systems lack commercially available experimental setup for wireless optogenetics, such as irradiation of high-power light at an optimal wavelength for specific molecular sensing, irradiation of multiple colors of visible light with independent temporal pattern, and irradiation of multiple animals or multiple sites within the same subject in parallel with independent temporal pattern.

Nevertheless, the potential of UCNP-based systems could be boosted in the future by improving the upconversion efficiency and application of different excitation wavelengths (745, 800, 980 nm, etc.), as well as developing multiple laser projection systems. Since UCNPs can also be printed on various substrates (even it is done three-dimensionally with a flexible pattern), their employment may stimulate deeper structures of the central and peripheral nervous systems with sophisticated spatiotemporal pattern in the near future. It is also important to describe the relativity of upconversion efficiency versus required power density and the possibility of rising temperature in tissues. Undoubtedly the most effective way to expand the application of UCNPs in optogenetic design and neuromodulation of

deeper structures in the central nervous system is to improve their efficiency.

Although UCNPs remain stable in nervous tissues, the long-term molecular and cellular effects of nanoparticle implantation on the neuronal population must be further investigated. One approach to mitigate the potential side effects is to design removable upconversion materials, which can be cleared from the nervous systems when the job is complete. One target is tapping the brain's immune system. This is achievable through chemokines that can be coated on the surface of current UCNPs. For example, UCNPs conjugated with chemokine (CCL21) are feasible to modulate T-cell migration.^[83] Another potential approach is to artificially control the physical displacements of UCNPs from the nervous system to the systemic circulation through means such as magnetic or electrical fields. The ability to completely remove injected nanoparticles from the nervous system will eliminate the potential side-effects and enhance the long-term biocompatibility effect for the nervous system. In addition, functional UCNPs that can cross the blood–brain barrier and target specific neuron populations shall also be considered, investigated, and introduced to NIR optogenetic studies.^[84] With such a nanoparticle neuron-targeting approach, stereotactic transplantation of UCNPs can be replaced with systemic intravenous injection, which will further reduce the invasiveness nature of the method.

5. Conclusion

Optogenetics has become a powerful tool for interrogating complex neuron networks. Incorporating upconversion materials into this technology offers the possibility of delivering light into the brain in an effective and minimally invasive manner. This technological advancement adds to the versatility of the current optogenetics toolbox. Upconversion emission has been validated both *in vitro* and *in vivo* to possess sufficient intensity to induce transmembrane depolarization in neurons. This success is built upon a deep-brain noncontact and biocompatible approach combined with the feasibility of surface modification of UCNPs. Critical factors that must be balanced include the upconversion efficiency and the issue of chronic biocompatibility. For this reason, the nanoparticle toxicity on the cellular, tissue, and organ levels must be systematically investigated to avoid particle-injection-induced loss of organ function. In addition, a quasi-continuous-wave laser excitation at 800 nm instead of 980 nm is recommended for optogenetic experiments to minimize heat generation. The successful application of NIR-optogenetics for neuromodulation would require advancements in multiple fields, including chemistry, materials science, nanotechnology, neuroscience, and optics.

Acknowledgements

This work was supported by the Singapore Ministry of Education (MOE2017-T2-2-110), Agency for Science, Technology and Research (A*STAR) (Grant No. A1883c0011), the National Research Foundation, Prime Minister's Office, Singapore under the NRF Investigatorship program (Award No. NRF-NRFI05-2019-0003), and the National Natural Science Foundation of China (21771135).

Conflict of Interest

The authors declare no conflict of interest.

Keywords

in vivo optogenetics, near-infrared light, noninvasive neuromodulation, upconversion nanoparticles

Received: June 1, 2018

Revised: June 12, 2019

Published online:

- [1] a) T. Ishizuka, M. Kakuda, R. Araki, H. Yawo, *Neurosci. Res.* **2006**, *54*, 85; b) K. Deisseroth, *Nat. Methods* **2011**, *8*, 26.
- [2] E. S. Boyden, F. Zhang, E. Bamberg, G. Nagel, K. Deisseroth, *Nat. Neurosci.* **2005**, *8*, 1263.
- [3] G. Nagel, T. Szellas, W. Huhn, S. Kateriya, N. Adeishvili, P. Berthold, D. Ollig, P. Hegemann, E. Bamberg, *Proc. Natl. Acad. Sci. USA* **2003**, *100*, 13940.
- [4] S. L. Jacques, *Phys. Med. Biol.* **2013**, *58*, R37.
- [5] F. Zhang, V. Gradinaru, A. R. Adamantidis, R. Durand, R. D. Airan, L. De Lecea, K. Deisseroth, *Nat. Protoc.* **2010**, *5*, 439.
- [6] K. Appasani, *Optogenetics: From Neuronal Function to Mapping and Disease Biology*, Cambridge University Press, Cambridge, UK **2017**, 132.
- [7] a) R. Weissleder, *Nat. Biotechnol.* **2001**, *19*, 316; b) A. M. Smith, M. C. Mancini, S. Nie, *Nat. Nanotechnol.* **2009**, *4*, 710.
- [8] J. Y. Lin, P. M. Knutsen, A. Muller, D. Kleinfeld, R. Y. Tsien, *Nat. Neurosci.* **2013**, *16*, 1499.
- [9] F. Zhang, M. Prigge, F. Beyrière, S. P. Tsunoda, J. Mattis, O. Yizhar, P. Hegemann, K. Deisseroth, *Nat. Neurosci.* **2008**, *11*, 631.
- [10] O. Yizhar, L. E. Fenno, M. Prigge, F. Schneider, T. J. Davidson, D. J. O'shea, V. S. Sohal, I. Goshen, J. Finkelstein, J. T. Paz, *Nature* **2011**, *477*, 171.
- [11] N. C. Klapoetke, Y. Murata, S. S. Kim, S. R. Pulver, A. Birdsey-Benson, Y. K. Cho, T. K. Morimoto, A. S. Chuong, E. J. Carpenter, Z. Tian, *Nat. Methods* **2014**, *11*, 338.
- [12] a) F. Wang, X. Liu, *Chem. Soc. Rev.* **2009**, *38*, 976; b) M. Haase, H. Schäfer, *Angew. Chem., Int. Ed.* **2011**, *50*, 5808; c) X. Qin, L. Shen, L. Liang, S. Han, Z. Yi, X. Liu, *J. Phys. Chem. C* **2019**, *123*, 11151; d) X. Qin, J. Xu, Y. Wu, X. Liu, *ACS Cent. Sci.* **2019**, *5*, 29; e) S. Wen, J. Zhou, K. Zheng, B. Artur, X. Liu, D. Jin, *Nat. Commun.* **2018**, *9*, 2415; f) L. Liang, Q. Xian, K. Zheng, X. Liu, *Acc. Chem. Res.* **2019**, *52*, 228.
- [13] a) H. Yawo, T. Asano, S. Sakai, T. Ishizuka, *Dev., Growth Differ.* **2013**, *55*, 474; b) S. Hososhima, H. Yuasa, T. Ishizuka, M. R. Hoque, T. Yamashita, A. Yamanaka, E. Sugano, H. Tomita, H. Yawo, *Sci. Rep.* **2015**, *5*, 16533.
- [14] G. Nagel, M. Brauner, J. F. Liewald, N. Adeishvili, E. Bamberg, A. Gottschalk, *Curr. Biol.* **2005**, *15*, 2279.
- [15] a) Z.-G. Ji, S. Ito, T. Honjoh, H. Ohta, T. Ishizuka, Y. Fukazawa, H. Yawo, *PLoS One* **2012**, *7*, e32699; b) R. B. Chang, D. E. Strochlic, E. K. Williams, B. D. Umans, S. D. Liberles, *Cell* **2015**, *161*, 622; c) E. Foster, H. Wildner, L. Tudeau, S. Haueter, W. T. Ralvenius, M. Jegen, H. Johannssen, L. Hösli, K. Haenraets, A. Ghanem, *Neuron* **2015**, *85*, 1289.
- [16] a) S. Zhao, J. T. Ting, H. E. Atallah, L. Qiu, J. Tan, B. Gloss, G. J. Augustine, K. Deisseroth, M. Luo, A. M. Graybiel, *Nat. Methods* **2011**, *8*, 745; b) L. Madisen, T. Mao, H. Koch, J.-m. Zhuo, A. Berenyi, S. Fujisawa, Y.-W. A. Hsu, A. J. Garcia III, X. Gu, S. Zanella, *Nat. Neurosci.* **2012**, *15*, 793.
- [17] a) O. Yizhar, L. E. Fenno, T. J. Davidson, M. Mogri, K. Deisseroth, *Neuron* **2011**, *71*, 9; b) B. Li, X.-y. Yang, F.-p. Qian, M. Tang, C. Ma, L.-Y. Chiang, *Brain Res.* **2015**, *1609*, 12.
- [18] a) H. Wang, Y. Sugiyama, T. Hikima, E. Sugano, H. Tomita, T. Takahashi, T. Ishizuka, H. Yawo, *J. Biol. Chem.* **2009**, *284*, 5685; b) G. Nagel, D. Ollig, M. Fuhrmann, S. Kateriya, A. M. Musti, E. Bamberg, P. Hegemann, *Science* **2002**, *296*, 2395.
- [19] X. Han, E. S. Boyden, *PLoS One* **2007**, *2*, e299.
- [20] A. Berndt, O. Yizhar, L. A. Gunaydin, P. Hegemann, K. Deisseroth, *Nat. Neurosci.* **2009**, *12*, 229.
- [21] a) X. Han, B. Y. Chow, H. Zhou, N. C. Klapoetke, A. Chuong, R. Rajimehr, A. Yang, M. V. Baratta, J. Winkle, R. Desimone, *Front. Syst. Neurosci.* **2011**, *5*, 18; b) V. Gradinaru, K. R. Thompson, K. Deisseroth, *Brain Cell Biol.* **2008**, *36*, 129.
- [22] T. Honjoh, Z.-G. Ji, Y. Yokoyama, A. Sumiyoshi, Y. Shibuya, Y. Matsuzaka, R. Kawashima, H. Mushiaki, T. Ishizuka, H. Yawo, *PLoS One* **2014**, *9*, e93706.
- [23] H. E. Covington, M. K. Lobo, I. Maze, V. Vialou, J. M. Hyman, S. Zaman, Q. LaPlant, E. Mouzon, S. Ghose, C. A. Tamminga, *J. Neurosci.* **2010**, *30*, 16082.
- [24] M. Hägglund, K. J. Dougherty, L. Borgius, S. Itoharu, T. Iwasato, O. Kiehn, *Proc. Natl. Acad. Sci. USA* **2013**, *110*, 11589.
- [25] W. J. Alilain, X. Li, K. P. Horn, R. Dhingra, T. E. Dick, S. Herlitze, J. Silver, *J. Neurosci.* **2008**, *28*, 11862.
- [26] a) I. Daou, A. H. Tuttle, G. Longo, J. S. Wieskopf, R. P. Bonin, A. R. Ase, J. N. Wood, Y. De Koninck, A. Ribeiro-da-Silva, J. S. Mogil, *J. Neurosci.* **2013**, *33*, 18631; b) L. W. Crock, B. J. Kolber, C. D. Morgan, K. E. Sadler, S. K. Vogt, M. R. Bruchas, R. W. Gereau, *J. Neurosci.* **2012**, *32*, 14217.
- [27] T. Asano, T. Ishizuka, H. Yawo, *Biotechnol. Bioeng.* **2012**, *109*, 199.
- [28] T. Bruegmann, D. Malan, M. Hesse, T. Beiert, C. J. Fuegeman, B. K. Fleischmann, P. Sasse, *Nat. Methods* **2010**, *7*, 897.
- [29] a) T. M. Reinbothe, F. Safi, A. S. Axelsson, I. G. Mollet, A. H. Rosengren, *Islets* **2014**, *6*, e28095; b) T. Kushibiki, S. Okawa, T. Hirasawa, M. Ishihara, *Gene Ther.* **2015**, *22*, 553.
- [30] S. Reardon, *Nature* **2016**, <https://doi.org/10.1038/nature.2016.20137>.
- [31] J. T. Paz, T. J. Davidson, E. S. Fretch, B. Delord, I. Parada, K. Peng, K. Deisseroth, J. R. Huguenard, *Nat. Neurosci.* **2013**, *16*, 64.
- [32] a) V. Gradinaru, M. Mogri, K. R. Thompson, J. M. Henderson, K. Deisseroth, *Science* **2009**, *324*, 354; b) A. V. Kravitz, B. S. Freeze, P. R. Parker, K. Kay, M. T. Thwin, K. Deisseroth, A. C. Kreitzer, *Nature* **2010**, *466*, 622.
- [33] K. Yamamoto, Z.-i. Tanei, T. Hashimoto, T. Wakabayashi, H. Okuno, Y. Naka, O. Yizhar, L. E. Fenno, M. Fukayama, H. Bito, *Cell Rep.* **2015**, *11*, 859.
- [34] I. B. Witten, S.-C. Lin, M. Brodsky, R. Prakash, I. Diester, P. Anikeeva, V. Gradinaru, C. Ramakrishnan, K. Deisseroth, *Science* **2010**, *330*, 1677.
- [35] a) A. R. Adamantidis, F. Zhang, A. M. Aravanis, K. Deisseroth, L. De Lecea, *Nature* **2007**, *450*, 420; b) A. M. Aravanis, L.-P. Wang, F. Zhang, L. A. Meltzer, M. Z. Mogri, M. B. Schneider, K. Deisseroth, *J. Neural Eng.* **2007**, *4*, S143.
- [36] G. Hong, S. Diao, J. Chang, A. L. Antaris, C. Chen, B. Zhang, S. Zhao, D. N. Atochin, P. L. Huang, K. I. Andreasson, *Nat. Photonics* **2014**, *8*, 723.
- [37] a) K. L. Montgomery, A. J. Yeh, J. S. Ho, V. Tsao, S. M. Iyer, L. Grosenick, E. A. Ferenczi, Y. Tanabe, K. Deisseroth, S. L. Delp, *Nat. Methods* **2015**, *12*, 969; b) J. G. McCall, T.-I. Kim, G. Shin, X. Huang, Y. H. Jung, R. Al-Hasani, F. G. Omenetto, M. R. Bruchas, J. A. Rogers, *Nat. Protoc.* **2013**, *8*, 2413; c) C. T. Wentz, J. G. Bernstein, P. Monahan, A. Guerra, A. Rodriguez, E. S. Boyden, *J. Neural Eng.* **2011**, *8*, 046021.
- [38] H. Ding, L. Lu, Z. Shi, D. Wang, L. Li, X. Li, Y. Ren, C. Liu, D. Cheng, H. Kim, *Proc. Natl. Acad. Sci. USA* **2018**, *115*, 6632.

- [39] a) J. O. Escobedo, O. Rusin, S. Lim, R. M. Strongin, *Curr. Opin. Chem. Biol.* **2010**, *14*, 64; b) K. Welscher, S. P. Sherlock, H. Dai, *Proc. Natl. Acad. Sci. USA* **2011**, *108*, 8943; c) Y. Zhang, G. Hong, Y. Zhang, G. Chen, F. Li, H. Dai, Q. Wang, *ACS Nano* **2012**, *6*, 3695; d) R. Wang, X. Li, L. Zhou, F. Zhang, *Angew. Chem., Int. Ed.* **2014**, *53*, 12086.
- [40] a) F. Auzel, *Chem. Rev.* **2004**, *104*, 139; b) Q. Chen, X. Xie, B. Huang, L. Liang, S. Han, Z. Yi, Y. Wang, Y. Li, D. Fan, L. Huang, *Adv. Biosyst.* **2019**, *3*, 1800233; c) Z. Wang, M. Hu, X. Ai, Z. Zhang, B. Xing, *Adv. Biosyst.* **2019**, *3*, 1800233; d) N. Yu, L. Huang, Y. Zhou, T. Xue, Z. Chen, G. Han, *Adv. Healthcare Mater.* **2019**, *8*, 1801132.
- [41] B. Zhou, B. Shi, D. Jin, X. Liu, *Nat. Nanotechnol.* **2015**, *10*, 924.
- [42] a) J. Shen, G. Chen, A. M. Vu, W. Fan, O. S. Bilsel, C. C. Chang, G. Han, *Adv. Opt. Mater.* **2013**, *1*, 644; b) X. Xie, N. Gao, R. Deng, Q. Sun, Q.-H. Xu, X. Liu, *J. Am. Chem. Soc.* **2013**, *135*, 12608; c) L. Liang, X. Xie, D. T. B. Loong, A. H. All, L. Huang, X. Liu, *Chem. - Eur. J.* **2016**, *22*, 10801.
- [43] a) G. S. Yi, G. M. Chow, *Adv. Funct. Mater.* **2006**, *16*, 2324; b) J. F. Suyver, J. Grimm, M. Van Veen, D. Biner, K. Krämer, H.-U. Güdel, *J. Lumin.* **2006**, *117*, 1.
- [44] a) F. Wang, X. Liu, *J. Am. Chem. Soc.* **2008**, *130*, 5642; b) Y. Zhang, L. Zhang, R. Deng, J. Tian, Y. Zong, D. Jin, X. Liu, *J. Am. Chem. Soc.* **2014**, *136*, 4893.
- [45] a) G. Tian, Z. Gu, L. Zhou, W. Yin, X. Liu, L. Yan, S. Jin, W. Ren, G. Xing, S. Li, *Adv. Mater.* **2012**, *24*, 1226; b) J. Wang, F. Wang, C. Wang, Z. Liu, X. Liu, *Angew. Chem.* **2011**, *123*, 10553.
- [46] L. Zhou, R. Wang, C. Yao, X. Li, C. Wang, X. Zhang, C. Xu, A. Zeng, D. Zhao, F. Zhang, *Nat. Commun.* **2015**, *6*, 6938.
- [47] F. Wang, R. Deng, J. Wang, Q. Wang, Y. Han, H. Zhu, X. Chen, X. Liu, *Nat. Mater.* **2011**, *10*, 968.
- [48] B. Zhou, W. Yang, S. Han, Q. Sun, X. Liu, *Adv. Mater.* **2015**, *27*, 6208.
- [49] Z. Li, Y. Zhang, S. Jiang, *Adv. Mater.* **2008**, *20*, 4765.
- [50] J. Lai, Y. Zhang, N. Pasquale, K. B. Lee, *Angew. Chem., Int. Ed.* **2014**, *53*, 14419.
- [51] S. Han, R. Deng, X. Xie, X. Liu, *Angew. Chem., Int. Ed.* **2014**, *53*, 11702.
- [52] M. Pollnau, D. R. Gamelin, S. Lüthi, H. Güdel, M. Hehlen, *Phys. Rev. B* **2000**, *61*, 3337.
- [53] a) W. Zou, C. Visser, J. A. Maduro, M. S. Pshenichnikov, J. C. Hummelen, *Nat. Photonics* **2012**, *6*, 560; b) X. Wu, H. Lee, O. Bilsel, Y. Zhang, Z. Li, T. Chen, Y. Liu, C. Duan, J. Shen, A. Punjabi, *Nanoscale* **2015**, *7*, 18424.
- [54] S. Heer, K. Kömpe, H. U. Güdel, M. Haase, *Adv. Mater.* **2004**, *16*, 2102.
- [55] G. Chen, H. Liu, H. Liang, G. Somesfalean, Z. Zhang, *J. Phys. Chem. C* **2008**, *112*, 12030.
- [56] a) D. J. Gargas, E. M. Chan, A. D. Ostrowski, S. Aloni, M. V. P. Altoe, E. S. Barnard, B. Sani, J. J. Urban, D. J. Milliron, B. E. Cohen, *Nat. Nanotechnol.* **2014**, *9*, 300; b) J. Zhao, D. Jin, E. P. Schartner, Y. Lu, Y. Liu, A. V. Zvyagin, L. Zhang, J. M. Dawes, P. Xi, J. A. Piper, *Nat. Nanotechnol.* **2013**, *8*, 729.
- [57] a) G.-S. Yi, G.-M. Chow, *Chem. Mater.* **2007**, *19*, 341; b) G. Chen, J. Damasco, H. Qiu, W. Shao, T. Y. Ohulchanskyy, R. R. Valiev, X. Wu, G. Han, Y. Wang, C. Yang, H. Ågren, P. N. Prasad, *Nano Lett.* **2015**, *15*, 7400; c) F. Vetrone, R. Naccache, V. Mahalingam, C. G. Morgan, J. A. Capobianco, *Adv. Funct. Mater.* **2009**, *19*, 2924.
- [58] a) Y. Zhang, L. Huang, X. Liu, *Angew. Chem., Int. Ed.* **2016**, *55*, 5718; b) H. Schäfer, P. Ptacek, O. Zerzouf, M. Haase, *Adv. Funct. Mater.* **2008**, *18*, 2913.
- [59] F. Wang, Y. Han, C. S. Lim, Y. Lu, J. Wang, J. Xu, H. Chen, C. Zhang, M. Hong, X. Liu, *Nature* **2010**, *463*, 1061.
- [60] Z. Li, Y. Zhang, *Nanotechnology* **2008**, *19*, 345606.
- [61] J.-C. Boyer, F. Vetrone, L. A. Cuccia, J. A. Capobianco, *J. Am. Chem. Soc.* **2006**, *128*, 7444.
- [62] H. Schäfer, P. Ptacek, K. Kömpe, M. Haase, *Chem. Mater.* **2007**, *19*, 1396.
- [63] J. Tian, X. Zeng, X. Xie, S. Han, O.-W. Liew, Y.-T. Chen, L. Wang, X. Liu, *J. Am. Chem. Soc.* **2015**, *137*, 6550.
- [64] M. Wang, G. Abbineni, A. Clevenger, C. Mao, S. Xu, *Nanomedicine* **2011**, *7*, 710.
- [65] J.-C. Boyer, M.-P. Manseau, J. I. Murray, F. C. van Veggel, *Langmuir* **2010**, *26*, 1157.
- [66] a) D. K. Chatterjee, A. J. Rufaihah, Y. Zhang, *Biomaterials* **2008**, *29*, 937; b) L. Xiong, Z. Chen, Q. Tian, T. Cao, C. Xu, F. Li, *Anal. Chem.* **2009**, *81*, 8687; c) J. Zhou, Z. Liu, F. Li, *Chem. Soc. Rev.* **2012**, *41*, 1323.
- [67] a) L. Cheng, K. Yang, M. Shao, X. Lu, Z. Liu, *Nanomedicine* **2011**, *6*, 1327; b) T. Cao, Y. Yang, Y. Sun, Y. Wu, Y. Gao, W. Feng, F. Li, *Biomaterials* **2013**, *34*, 7127; c) Y. Sun, W. Feng, P. Yang, C. Huang, F. Li, *Chem. Soc. Rev.* **2015**, *44*, 1509.
- [68] R. Chen, G. Romero, M. G. Christiansen, A. Mohr, P. Anikeeva, *Science* **2015**, 1261821.
- [69] S. Shah, J.-J. Liu, N. Pasquale, J. Lai, H. McGowan, Z. P. Pang, K.-B. Lee, *Nanoscale* **2015**, *7*, 16571.
- [70] X. Wu, Y. Zhang, K. Takle, O. Bilsel, Z. Li, H. Lee, Z. Zhang, D. Li, W. Fan, C. Duan, E. M. Chan, C. Lois, Y. Xiang, G. Han, *ACS Nano* **2016**, *10*, 1060.
- [71] F. B. Shipley, C. M. Clark, M. J. Alkema, A. M. Leifer, *Front. Neural Circuits* **2014**, *8*, 28.
- [72] a) A. Bansal, H. Liu, M. K. G. Jayakumar, S. Andersson-Engels, Y. Zhang, *Small* **2016**, *12*, 1732; b) X. Ai, L. Lyu, Y. Zhang, Y. Tang, J. Mu, F. Liu, Y. Zhou, Z. Zuo, G. Liu, B. Xing, *Angew. Chem., Int. Ed.* **2017**, *56*, 3031.
- [73] X. Lin, Y. Wang, X. Chen, R. Yang, Z. Wang, J. Feng, H. Wang, K. W. Lai, J. He, F. Wang, *Adv. Healthcare Mater.* **2017**, *6*, 1700446.
- [74] Y. Wang, X. Lin, X. Chen, X. Chen, Z. Xu, W. Zhang, Q. Liao, X. Duan, X. Wang, M. Liu, F. Wang, J. He, P. Shi, *Biomaterials* **2017**, *142*, 136.
- [75] S. Chen, A. Z. Weitemier, X. Zeng, L. He, X. Wang, Y. Tao, A. J. Huang, Y. Hashimoto-dani, M. Kano, H. Iwasaki, *Science* **2018**, *359*, 679.
- [76] T. Miyazaki, S. Chowdhury, T. Yamashita, T. Matsubara, H. Yawo, H. Yuasa, A. Yamanaka, *Cell Rep.* **2019**, *26*, 1033.
- [77] Y. Ma, J. Bao, Y. Zhang, Z. Li, X. Zhou, C. Wan, L. Huang, Y. Zhao, G. Han, T. Xue, *Cell* **2019**, *177*, 243.
- [78] L. He, Y. Zhang, G. Ma, P. Tan, Z. Li, S. Zang, X. Wu, J. Jing, S. Fang, L. Zhou, Y. Wang, Y. Huang, P. G. Hogan, G. Han, Y. Zhou, *eLife* **2015**, *4*, e10024.
- [79] X. Lin, X. Chen, W. Zhang, T. Sun, P. Fang, Q. Liao, X. Chen, J. He, M. Liu, F. Wang, P. Shi, *Nano Lett.* **2018**, *18*, 948.
- [80] B. Zheng, H. Wang, H. Pan, C. Liang, W. Ji, L. Zhao, H. Chen, X. Gong, X. Wu, J. Chang, *ACS Nano* **2017**, *11*, 11898.
- [81] K. Montgomery, A. Yeh, J. Ho, V. Tsao, S. Iyer, L. Grosenick, E. Ferenczi, Y. Tanabe, K. Deisseroth, S. Delp, *Nat. Methods* **2015**, *12*, 969.
- [82] S. Park, D. Brenner, G. Shin, C. Morgan, B. Copits, H. Chung, M. Pullen, K. Noh, S. Davidson, S. Oh, *Nat. Biotechnol.* **2015**, *33*, 1280.
- [83] K. Lee, E. Seow, Y. Zhang, Y. Lim, *Biomaterials* **2013**, *34*, 4860.
- [84] D. Ni, J. Zhang, W. Bu, H. Xing, F. Han, Q. Xiao, Z. Yao, F. Chen, Q. He, J. Liu, *ACS Nano* **2014**, *8*, 1231.